Journal of Materials Chemistry C

Accepted Manuscript

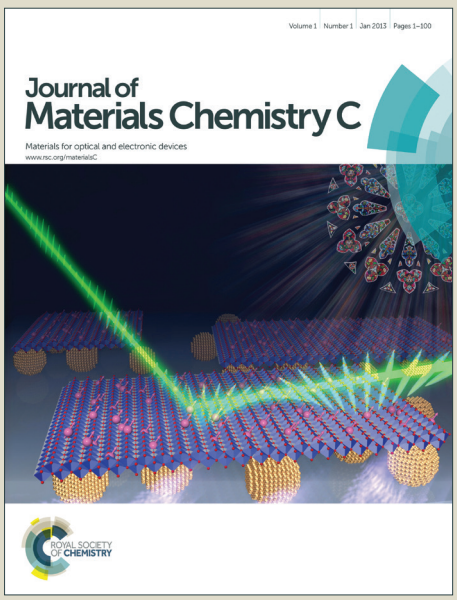

ROYAL SOCIETY OF CHEMISTRY

www.rsc.org/materialsC

Journal of Materials Chemistry C

ARTICLE

The Crucial Role of Self-assembling in Nonlinear Optical Properties of Polymeric Composites Based on Crown-substituted Ruthenium Phthalocyaninate

Received 00th January 20xx,
Accepted 00th January 20xx

DOI: 10.1039/x0xx00000x

www.rsc.org/

Yulia G. Gorbunova[ab*], Antonina D. Grishina[a], Alexander G. Martynov[a], Tatiyana V. Krivenko[a], Alexandra A. Isakova[a], Vladimir V. Savel'ev[a], Sergey E. Nefedov[b], Eugeny V. Abkhalimov[a], Anatoly V. Vannikov[a], Aslan Yu. Tsivadze[ab]

Ruthenium(II) tetra-15-crown-5-phthalocyaninate with axially coordinated molecules of pyrazine $[(15C5)_4Pc]Ru(pyz)_2$ (**1**) was synthesized from carbonyl complex $[(15C5)_4Pc]Ru(CO)(MeOH)$ (**2**),and the structure of the solvate complex (**1**)·$6CHCl_3$ was revealed by the single crystal X-ray diffraction method. Analysis of crystal packing shows the essential role of weak intermolecular interactions, such as CH…π, CH…N, CH…O and CH…Cl, in the formation of stable assemblies and their organization within the crystals. The interplay between the *intramolecular* axial coordinated pyrazine contacts and weak *intermolecular* interactions of solvate molecules with crown-ether fragments provides the basis for rationalizing the observed self-assembling of molecules in solutions of tetrachloroethane and polymeric composites with polyvinylcarbazole. The self-assembling was investigated by means of UV-Vis spectroscopy, dynamic light scattering measurements, AFM and TEM techniques. The formation of nanoparticles of complex (**1**) from a tetrachloroethane solution after three cycles of heating to 70°C/cooling to 5°C and 2-days storage was proved. Thin films (7 μm) of polymeric composites with polyvinylcarbazole prepared from solution containing nanoparticles exhibit nonlinear optical response measured by the Z-scan technique with application of femtosecond (1030 nm) and nanosecond (1064 nm) pulse lasers. The measured third-order susceptibility ($\chi^{(3)}$) of the polyvinylcarbazole composite with 4 wt% of complex (**1**) is equal to 1.94×10^{-10} esu, while the same composite prepared without the above-described special treatment has zero susceptibility. This result proves the essential role of self-assembling in further development of nonlinear optical materials.

[a]*Frumkin Institute of Physical Chemistry and Electrochemistry, Russian Academy of Sciences, Leninskiy Pr. 31, Moscow, 119071, Russia*
[b]*Kurnakov Institute of General and Inorganic Chemistry, Russian Academy of Sciences, Leninskiy Pr. 31, Moscow, 119991, Russia*
e-mail: yulia@igic.ras.ru

† Footnotes relating to the title and/or authors should appear here.
Electronic Supplementary Information (ESI) available: a scheme of the *Z*-scan measurement technique, molecular structure of complex (**1**), crystal packing of complex (**1**). See DOI: 10.1039/x0xx00000x

INTRODUCTION

Synthesis of compounds with nonlinear optical properties (NLO) is related to the search for the systems that limit the intensity of laser irradiation in nanoseconds and shorter time and thereby protect photosensitive devices and the eye from strong radiation. Among organic components of nonlinear optical materials, phthalocyanines (Pc) constitute one of the most attractive classes of photosensitizers,[1,2] whose strong nonlinearities arise from highly delocalized 18π-electron aromatic systems. Variation of substituents at the periphery of the Pc macrocycle, as well as the metal ion in its cavity and axial ligands, results in the appearance of a huge family of compounds, affording thereby fine tuning of required physicochemical characteristics. Even larger diversity of properties can be achieved by means of supramolecular assembly of Pc molecules giving extended aggregates with enhanced nonlinear susceptibility. This effect appears both in solutions of aggregated Pc's[3,4] and in films obtained by various techniques – cast, epitaxial growth, spin-coating, Langmuir-Blodgett, etc.[3,5–7] To produce materials, incorporation of Pc's into a polymeric matrix is also widely used.[3,8–10] Formation of such composites typically results in enhancement of nonlinear optical properties of phthalocyanines,[11–15] as well as improves their photo- and thermal stability as compared to the same Pc's molecules in solution.[10]

Among the substituted phthalocyanines, crown-ether derivatives are very promising building blocks for assembly of molecules into cofacial and brick-wall supramolecular structures.[16,17] Study of crown-substituted phthalocyanines has attracted attention due to the development, on their basis, of photorefractive materials, molecular switches and redox-active compounds, as well as sensors for cations and anions and nonlinear optical materials.[18–25] It has been established earlier that the photoelectric and photorefractive properties of the polymer composites consisting of Ru(II) crown-phthalocyanines with axially coordinated 1,4-diazabicyclo[2.2.2]octane(DABCO) molecules are enhanced by the formation of supramolecular assemblies.[18,26] The third-order nonlinear optical properties of this ruthenium(II) complex have been measured by means of Z-scan techniques in a tetrachloroethane (TCE) solution. It has been found that the third-order molecular polarizability per molecule increases by a factor of 3.6 in going from single molecules to the supramolecular assembly formed in solution during heating/cooling cycles.[27] The morphology of these assemblies was investigated using atomic force microscopy, which demonstrated the presence of stable supramolecular wires 7–8 nm in height, 100–150 nm in width and 600 nm or more in length.[18] All previous studies of crown-Pc nonlinear optical properties have been performed in solution while the NLO behavior in the solid state is very important for the development of optical devices. It is also known that changing the nature of axial ligands in MPc's leads to a considerable enhancement in optical limiting response[9]. Taking all these into account, we report here features of self-assembling and the optical behavior of composites of ruthenium(II) tetra-15-crown-5-phthalocyaninate containing axially coordinated molecules of pyrazine $[(15C5)_4Pc]Ru(pyz)_2$ (**1**) with polyvinylcarbazole (PVC) measured by the Z-scan technique. The molecular and supramolecular structures of complex (**1**) in the solid state were described using single-crystal X-ray diffraction data. The composition and morphology of supramolecular assemblies formed in a tetrachloroethane solution were studied by means of transmission electron microscopy and atomic force microscopy (TEM and AFM), as well as UV-Vis spectroscopy and dynamic light scattering (DLS).

EXPERIMENTAL SECTION

Materials

Pyrazine, tetrachloroethane, methanol, o-dichlorobenzene (o-DClB), polyvinylcarbazole (glass transition point of 200°C) and $Me_3NO{\cdot}2H_2O$ were available from commercial suppliers (Acros, Merck, Aldrich, Sigma). Chloroform (CHIMMED, stabilized with 0.6-1% EtOH) was dried over $CaCl_2$ and distilled over CaH_2. Neutral alumina (Merck) was used for column chromatography. Phthalocyanine $[(15C5)_4Pc]Ru(CO)(MeOH)$ (**2**) was synthesized by the previously reported method.[28]

Synthesis of Bis(pyrazine)(tetra-15-crown-5-phthalocyaninato)ruthenium(II) (1)

A mixture of $[(15C5)_4Pc]Ru(CO)(MeOH)$ **(2)** (17.4 mg, 12.1 μmol), $Me_3NO{\cdot}2H_2O$ (5.4 mg, 48.5 μmol) and 500 mg of pyrazine in 3 ml of $CHCl_3$ was refluxed for 1 h until the Q-band of carbonyl the complex (655 nm) vanished in the UV-Vis spectrum of a reaction mixture sample. After cooling to room temperature, the mixture was poured into hexane (50 ml), the resulting dark blue precipitate was filtered off and chromatographed on neutral alumina. Elution with $CHCl_3$+0-2vol.% MeOH afforded 16.8 mg (~90%) of a mixture containing the target complex $[(15C5)_4Pc]Ru(pyz)_2$ (**1**) together with 15 mol% of the heteroligand complex $[(15C5)_4Pc]Ru(pyz)(Me_3N)$ **(1a)** as evidenced by NMR. To remove the side product, the mixture of complexes was dissolved in 3 ml of *o*-dichlorobenzene, 125 mg of pyrazine was added, and the solution was refluxed for 15 min under a slow argon flow. After cooling to room temperature, the mixture was poured into hexane (50 ml), and the dark blue precipitate was filtered and dried. Its NMR investigation was evidence of the complete substitution of axially coordinated trimethylamine with pyrazine.

^{1}H NMR (600 MHz, $CDCl_3$) δ, ppm: 8.59 (s, 8H, H_{Pc}), 6.46 (d, *J* = 4.5 Hz, 4H, *m*-Pyz), 4.69 (m, 16H, α-OCH_2), 4.17 (m, 16H, β-OCH_2), 3.90 (m, 32H, γ,δ-OCH_2), 2.38 (d, *J* = 4.5 Hz, 4H, *o*-Pyz). UV-Vis (λ_{max}, nm (lgε)): 631 (4.79) 576 sh. 362 (4.54) 322 (5.15), IR (ν, cm^{-1}): 2867 (w), 1606 (w), 1583 (m), 1445 (m), 1471 (m), 1447 (m), 1399 (m), 1373 (m), 1227 (vs), 1201 (m), 1148 (m), 1109 (vs), 1066 (s), 979 (vs), 936 (s), 906 (m), 860 (m), 817(s), 735(s); HR MS (ESI) calcd. for $C_{72}H_{81}N_{12}NaO_{20}Ru$ $[M+H+Na]^{2+}$ 779.232; found 779.230.

Characterization

NMR spectra were recorded on a BrukerAvance 600 spectrometer. NMR spectra were referenced against the residual proton signals of the deuterated solvent.[29] UV-Vis spectra were measured with a Varian Cary-100 and on a Shimadzu UV-3101PC spectrophotometers in quartz cells with 10-mm optical path. An FT-IR Nexus (Nicolet) spectrometer with a micro-ATR accessory (Pike) was used to record IR spectra. Accurate mass measurements (HR ESI-MS) were performed on Bruker Maxis Impact mass spectrometer. Solutions in CHCl3/methanol (1:1) were used for the analysis. Samples for AFM were prepared by casting of 5 μl of 7 $\times 10^{-4}$ M solution in TCE onto freshly peeled mica surface. The AFM investigation was carried out with an AFM model Enviroscope and a Nanoscope V controller from Bruker Company. Image acquisition was performed in the tapping mode. Cantilevers NSG 01 (resonance frequency 150 kHz, force constant 5.5 Nm^{-1}, curvature radius 10 nm; NT-MDT Corporation (Russia, Moscow) were used. Data were processed by WSxM 4.11 software (Nanotec Electronica, Spain, Madrid).[30]

Transmission electron microscopy (TEM) images and selected area electron diffraction (SAED) patterns were obtained on a Carl Zeiss LEO912 AB OMEGA (Carl Zeiss) TEM instrument operating at 100 kV. Before analysis by TEM, the solution of complex (1) was dripped onto a carbon-coated copper grid and air-dried at room temperature.

The size of nanoparticles in the solution was determined by dynamic light scattering (DLS) technique. Prior to the measurements, solutions were thermostated at 20°C. The measurements were carried out in a quartz cell on a Delsa Nano C particle analyzer (Beckman Coulter, United States) at a wavelength of 658 nm using the Delsa Nano v.3.73 software package. The average particle sizes were obtained from particle size distributions calculated from the autocorrelation functions of scattering intensity by the CONTIN method.

X-ray structure analysis

Dark blue crystals of solvate $[(15C5)_4Pc]Ru(pyz)_2{\cdot}6CHCl_3$ were obtained by slow evaporation of its solution in $CHCl_3$. Single-crystal X-ray diffraction experiments were carried out on a Bruker SMART APEX II diffractometer with a CCD area detector (graphite monochromator, Mo-Kα radiation, λ = 0.71073 Å, ω-scans). a = 12.3589(11) Å, b = 14.0410(12) Å, c = 14.1355(12) Å, α = 96.287(2)°, β = 104.6120(10)°, γ = 102.610(2)°, V = 2280.9(3) $Å^3$ (150K), Z = 1, D_{calc} = 1.639 g/cm^3, 25204 measured reflections, 12016 [R(int) = 0.0774] independent reflections with $F^2 > 2\sigma(I)$, μ = 0.479 cm^{-1}, R_1= 0.0710, wR_2 = 0.1519. The semi-empirical method SADABS[31] was applied for absorption correction. The structures were solved by direct methods and refined by the full-

matrix least-squares technique on F^2 with anisotropic displacement parameters for all non-hydrogen atoms. All the hydrogen atoms in the complexes were placed geometrically and included in the structure factor calculation in the riding motion approximation. All the data reduction and further calculations were performed using the SAINT[32] and SHELXTL-97[33] program packages. The CCDC reference number is 1056316. The data can be obtained free of charge from the Cambridge Crystallographic Data Centre at www.ccdc.cam.ac.uk/data_request/cif

Composite fabrication and Z-scan measurements

Solution of complex **(1)** in tetrachloroethane (c = 7 × 10^{-4} mol/L) was heated to 70°C and cooled to 5°C with simultaneous measurements of UV-Vis spectra in the 400-1400 nm range. Heating-cooling cycles were repeated for three times. For preparation of polymeric composites, polyvinylcarbazole (Aldrich, MW = 1.1 × 10^6, glass transition temperature 200°C) was added to the thermally treated and aged for 48 h solution (4% wt of complex **(1)**), and the mixture was agitated with a magnetic stirrer. The obtained viscous solution was poured onto a polyethylene transparent film fixed in a frame and dried on a heating plate. After evaporation of the solvent, the thickness of the composite was measured with an interferometer: the layer thickness was 7 μm. Nonlinear optical characteristics were determined by the Z-scan technique with an Origami-10 femtosecond laser (1030 nm) and a Nd:YAG nanosecond pulse laser (1064 nm). The pulse length of the femtosecond laser was 217 fs with a rate of 74.82×10^6 s^{-1} and an average laser light power of 0.15 J/s. An energy of light per pulse was 2 × 10^3 J with total power I = 0.15/(74.82×10^6 ×217×10^{-15}) = 9.24×10^3 W. The diameter of the laser beam at the focal point was 20.6 μm, and the light intensity at the lens focal point was $I_0 = I/(\pi w_0^2)$ = 6.92×10^8 W/cm^2. Femtosecond laser beam was opened for ~ 470 μs; the rise time of the signal in the initial period was about 10 μs. Measurements were carried out by irradiation of the sample for 40 μs and 450 μs. The nanosecond laser emits a train of five 10-ns pulses with a total intensity of 0.75 W. A holder with polymeric composite was moved along the beam direction from –z to +z range, the light transmittance through the sample was measured in two modes, namely, closed-aperture transmittance (T_{CA}) or open-aperture transmittance (T_{OA}) (Fig. S1).

Results and discussion

Synthesis

Ruthenium(II) tetra-15-crown-5-phthalocyaninate with axially coordinated pyrazine molecules, $[(15C5)_4Pc]Ru(pyz)_2$ **(1)**, was synthesized starting from the previously described carbonyl complex $[(15C5)_4Pc]Ru(CO)(MeOH)$ **(2)**.[28] To this end, complex **(2)** was treated with trimethylamine N-oxide in the presence of excess pyrazine in refluxing chloroform.[34] It resulted in formation of a mixture of two decarbonylated complexes – target complex **(1)** and the side product with axially coordinated pyrazine and trimethylamine ligands $[(15C5)_4Pc]Ru(pyz)(NMe_3)$ **(1a)** in a 85/15 ratio as evidenced by NMR (Scheme 1). To avoid tedious chromatographic separation of these complexes, this mixture was refluxed in *o*-dichlorobenzene in the presence of excess pyrazine. Due to the high boiling point of *o*-DClB (180°C), volatile trimethylamine was removed from the Ru(II) coordination sphere and was replaced with pyrazine, affording pure target complex **(1)**.

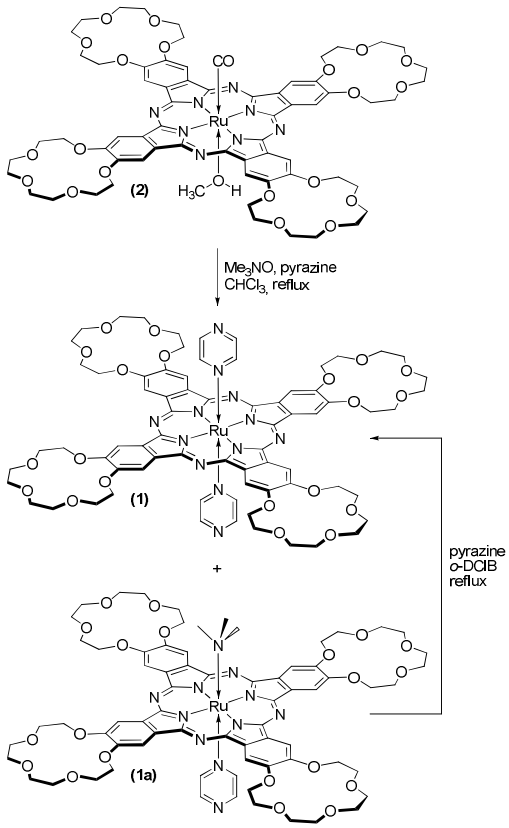

Scheme 1.

X-Ray diffraction analysis

Single crystals of complex **(1)** suitable for X-ray diffraction analysis were obtained by slow evaporation of a solution of the complex in $CHCl_3$.

It was found that, in the centrosymmetric molecule, the Ru(II) atom has an octahedral environment formed by four isoindole nitrogen atoms belonging to the phthalocyanine macrocycle [the Ru – N_{iso} distances are 1.984(4) – 1.999(4) Å] and two nitrogen atoms from the coordinated pyrazine molecules [Ru – N_{pyz} = 2.089(4) Å] (Fig.1, S2). Both pyrazine molecules are located in the same plane that includes *meso*-nitrogen atoms line N(4)/N(4A) and ruthenium atom. This plane is almost orthogonal to the phthalocyanine plane [tilt angle is 5.1°]. This arrangement of pyrazine molecules might be caused by formation of relatively short intramolecular hydrogen bonds and CH…π contacts of carbons atoms C(33) and C(36) with carbon and nitrogen atoms of six-members cycle of phthalocyanine Ru-N(1A)-C(32)-N(4)-C(31)-N(3) [C…C contacts are 3.382-3.480 Å; N…C contacts are 3.093-3.211Å]. From the other hand such geometry can be caused by intermolecular CH…O contacts of these atoms as well as carbon atoms C(34) and C(35) with oxygen atoms O(3) and O(8) of the crown ether substituents of other complex **(1)** located in crystal cell [C…O contacts are 3.174-3.337 Å] (Fig. 1 and S3).

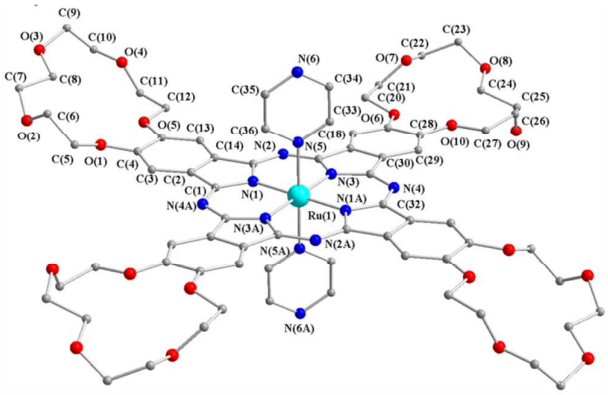

Fig.1 Molecular structure of complex **(1)**. Hydrogen atoms are omitted for clarity.

Notably, the Ru – N_{pyz} distance is significantly shorter than the one observed in the similar crystal structure of $[(15C5)_4Pc]Ru(DABCO)_2$ reported previously[35] [Ru – N_{DABCO} = 2.244(3) Å], suggesting stronger binding of the aromatic ligand in comparison with the aliphatic amine. Apparently, this stronger binding is a reason of the successful substitution of the NMe_3 ligand with pyrazine at elevated temperature.

The molecules of complex form a brickwall-like 3D packing where the planes of all phthalocyanine macrocycles are parallel to each other (Fig.S3). Each molecule of the complex is surrounded by eight other molecules. Such a packing is a result of weak but multiple intermolecular interactions dominated by contacts with crown-ether macrocycles. Their oxygen atoms form CH...O contacts with the pyrazine moiety as described above. In addition, OCH_2 moieties are involved in formation of weak intermolecular hydrogen bonds with pyrazine nitrogen atoms and phthalocyanine *meso*-N atoms. Finally, multiple CH...π contacts are formed by the OCH_2 groups and benzene moieties of the phthalocyanine ring. It should be mentioned that pyrazine molecules do not form stacking contacts with each other or with other π-systems.

The voids between the molecules are filled with $CHCl_3$ molecules, forming therefore the **(1)**·$6CHCl_3$ solvate. Notably, four chloroform molecules forms hydrogen bonds with only one of oxygen atom of crown-ether macrocycle [C(37)…O(2) 3.126; C(38)…O(4) 3.134 (Fig. 2)], in contrast to the crystal lattice of $[(15C5)_4Pc]Ru(DABCO)_2·7CHCl_3$ or sandwich lanthanide complexes where at least four oxygen atoms of crown ethers are involved in binding with chloroform.[35–37] This might be explained by numerous weak CH...Cl contacts of $CHCl_3$ molecules with phthalocyanine aromatic protons. Solvate $CHCl_3$ forms clusters constructed of six molecules combined through Cl...Cl contacts [3.42 – 3.47 Å].[38]

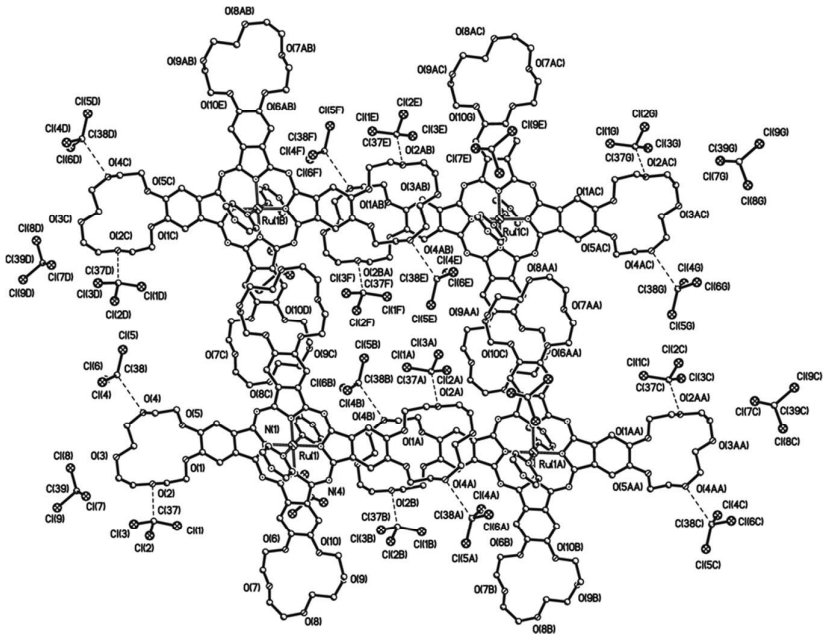

Fig.2 Crystal packing of **(1)**·6$CHCl_3$ solvate. Hydrogen atoms are omitted for clarity.

Thus, the obtained X-ray data have demonstrated that possible multiple weak intermolecular interactions within the crown-ether substituted phthalocyanines are playing key role not only in single crystal growth but, in general, such interactions are responsible for the complex geometry as well as crystal packing of molecules.

Assembly in solution and thin films

The measurements of UV-Vis spectra of **(1)** dissolved in TCE upon heating and cooling procedure were taken with a spectrophotometer equipped with a Peltier cell. Being in the monomeric state, complex **(1)** revealed a single Q-band at 634 nm in the UV-Vis spectrum of the solution (Fig. 3). After three cycles of heating this solution to 70°C and slow cooling to 5°C, the Q-band was broadened with simultaneous decrease in intensity, which corresponds to aggregation of molecules. A similar behavior was observed previously for other crown-phthalocyaninates.[16,17]

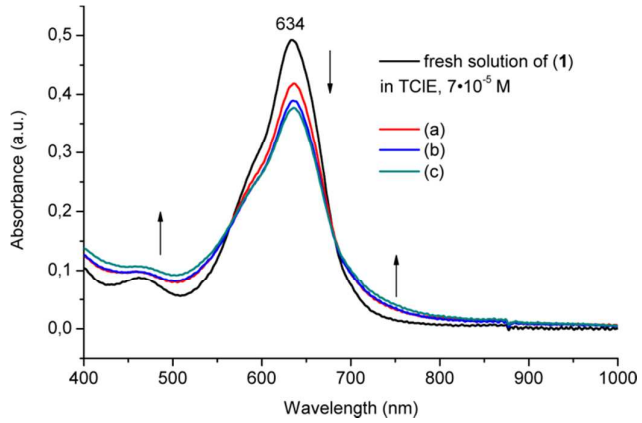

Fig.3 Q-band region of UV-Vis spectra of a solution of **(1)** in TCE before and after the first (a), second (b) and third (c) cycle of heating to 70°C and cooling to 5°C.

The simultaneous DLS measurements after the first heating/cooling cycle revealed formation of nanoparticles with the average size 1.5±0.4 nm (Fig.4), which were absent in the fresh solution. One more heating/cooling cycle resulted in further aggregation of complex **(1)** which was followed by a decrease in intensity of the Q-band (Fig.3), as well as in negligible growth of nanoparticle size. The third heating/cooling cycle did not result in dramatic changes of UV-Vis spectra and the size of nanoparticles, suggesting that the formation of nanoparticles was essentially finished during the second heating/cooling cycle. Notably, the obtained colloidal system was unstable, and the size of nanoparticles continued to grow with time during storage of the solution. Thus, the DLS profile after the storage of the thermally treated solution for 12 h at room temperature indicates that such aging of sample gives rise to spontaneous self-assembling of molecules with formation of 50.4±17.6 nm particles; after storage for 48 h, the solution contains particles with the average size 213±55.2 nm (Fig.4). It should be noted that similar storage of a thermally untreated solution did not lead to the formation of such assemblies. Therefore, simultaneous application of UV-Vis spectroscopy and DLS measurements demonstrates the formation of supramolecular assemblies by **(1)** in TCE solutions after the above thermal treatment and further storage of this solution.

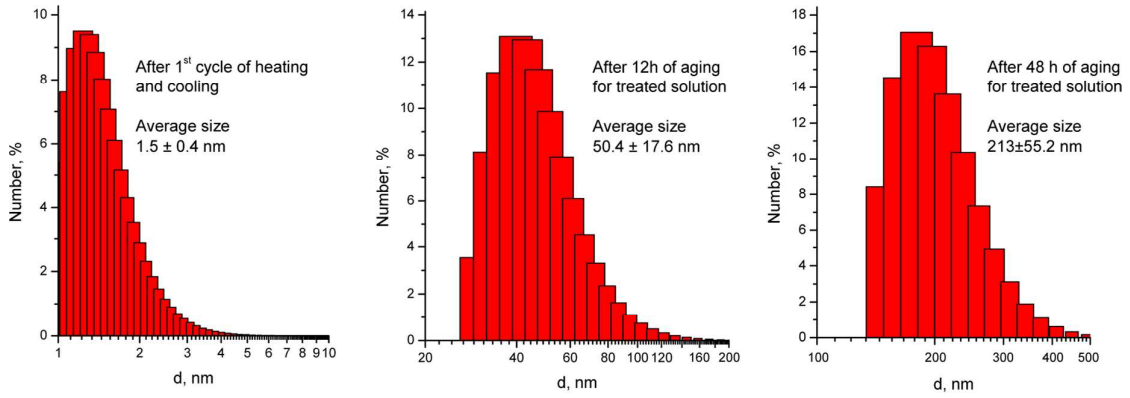

Fig. 4 Histograms of particle size distributions of 7×10^{-5} M complex **(1)** in TCE solution, obtained by DLS .

The investigation of assembling of molecules in thin solid films is also very important for finding peculiarities of the complex behavior during the composite preparation. For this purpose, the morphology of cast films obtained from a freshly prepared solution of complex **(1)** and from thermally treated solutions was studied by AFM and TEM. Figure 5 demonstrates the images of $[(15C5)_4Pc]Ru(pyz)_2$ cast films on the mica surface. AFM studies of the cast film obtained from a freshly prepared solution of complex **(1)** on mica did not reveal the formation of large particles. Indeed, the cylindrical particles of approximately 10 nm in height were observed (Fig.5a-c). However, when a solution of complex **(1)** in TCE was heated and cooled for three times and cast on the mica surface, the formation of large cubic aggregates was observed by AFM (Fig.5d-f). The average size of these aggregates was 400x200 nm. Taking into account single-crystal X-ray diffraction data, we can assume that molecules of TCE take part in the self-assembly of molecules **(1)** to give brick-wall structures.

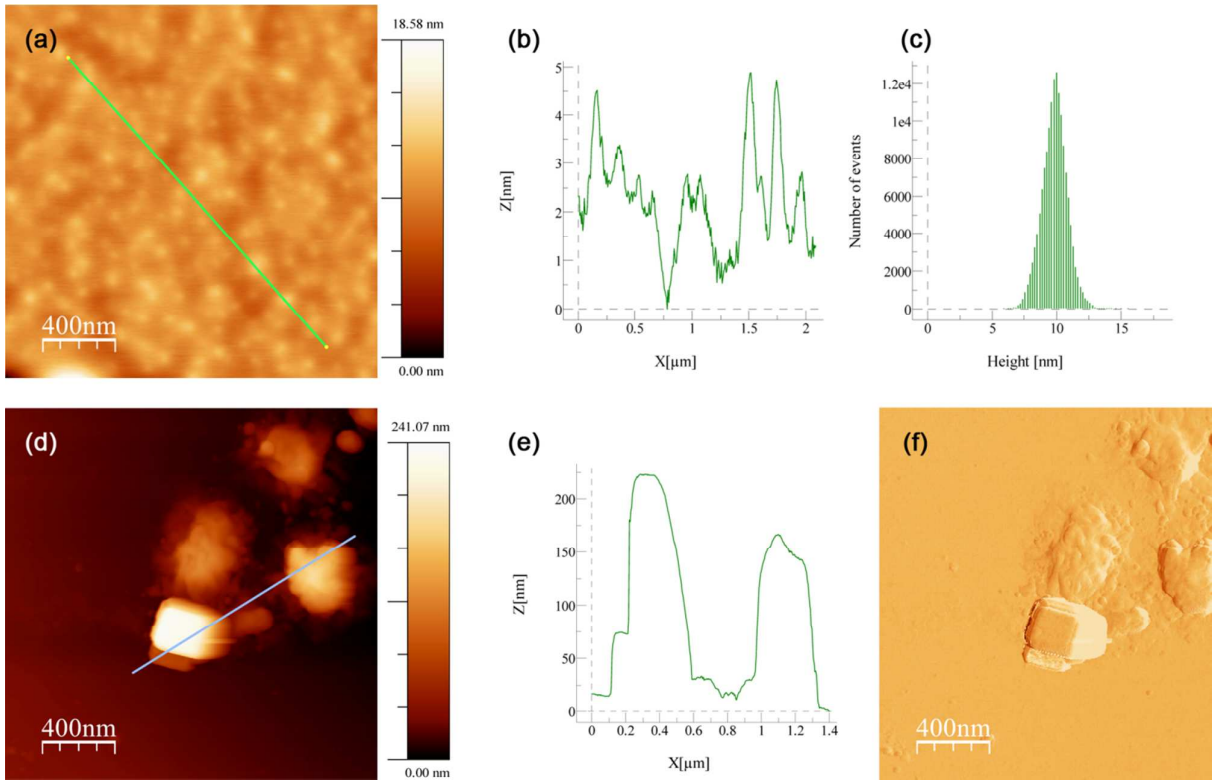

Fig.5AFM images of complex **(1)**: *(a)* – cast film prepared from a fresh solution (7×10^{-4} M); *(b)* – line profile showing the size of the particles; (c) – histogram showing the height of the particles; *(d)* – cast film prepared from the thermally treated solution (3 cycles); *(e)* - line profile showing the size of the crystals; (f) – phase image of crystals .

Moreover, the formation of such assemblies results in appearance of an electron diffraction pattern with strong reflections in TEM images, which is evidence of their crystalline nature (Fig.6). It should be noted that the cast film prepared for TEM from a fresh solution did not give rise to electron diffraction due to the amorphous nature of particles.

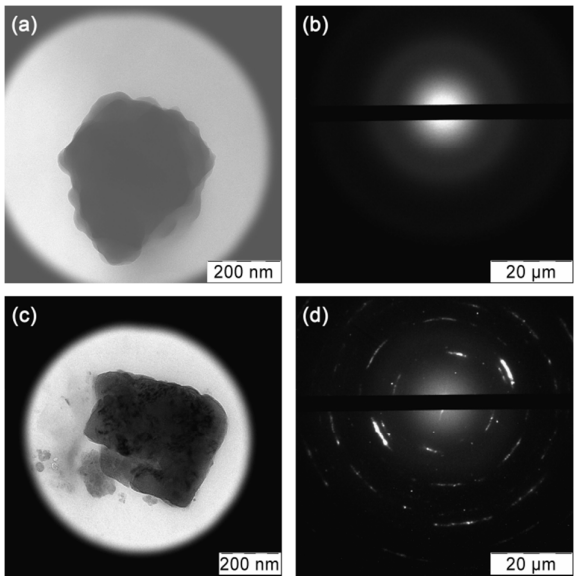

Fig.6 TEM images of complex **(1)**: *(a)* – cast film prepared from a fresh solution (7×10^{-4} M) on graphite surface; *(b)* – electron diffraction pattern from the film (a); *(c)* –cast film prepared from a thermally treated solution on graphite surface; *(d)* – electron diffraction pattern from the film (c).

Finally, in order to understand the assembling behavior of complex **(1)** in the polymeric composite, we investigated the UV-Vis spectra of the PVC composite with **(1)** (4 wt %). Figure 7a shows the spectrum of the PVC-**(1)** composite prepared from a fresh solution in TCE. The typical broadening of the Q-band of a solid sample in the comparison with that of a solution occurs without any shift of the band. In contrast, when a film is prepared from a thermally treated solution, the red shift of the Q-band with additional absorption up to 1400 nm occurs, which correlates with the formation of brick-wall assemblies of phthalocyanines (Fig.7b).[39,40] It was shown earlier that namely such assemblies in polymeric composites were responsible for the photorefractive properties of ruthenium phthalocyanine in near-IR spectral range.[26,27]

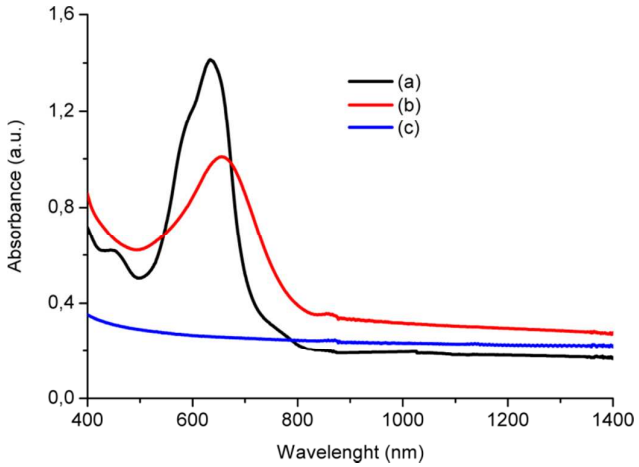

Fig.7 UV-Vis spectra of the PVC composite with complex (**1**) (4 wt %). The 7 μm thick film was prepared from a fresh solution of complex **(1)** in TCE (*a*) and from a solution subjected to three cycles of heating to 70°C and slow cooling to 5°C *(b);* UV-Vis spectra of a PVC film without the complex *(c).*

Z-scan measurement of the optical nonlinearity of composites

At the high intensity of laser irradiation in the Rayleigh range, the volume polarization of the sample P(E) is significantly contributed to the nonlinear components. In a solution or polymeric film at random centrosymmetric orientation of nonlinear chromophores, the second-order susceptibility vanishes to zero and $P(E) = \chi^{(1)}E + \chi^{(3)}E^3$ (E is the electric field of an electromagnetic wave, $\chi^{(1)}$ is the linear susceptibility and $\chi^{(3)}$ is the third-order susceptibility).

As $n^2 = 1 + 4\pi P/E$, hence in Equation 1:

$n = (1 + 4\pi\chi^{(1)})^{0.5}\times\{1 + [4\pi\chi^{(3)}E^2/(1 + 4\pi\chi^{(1)})]\}^{0.5} = (1 + 4\pi\chi^{(1)})^{0.5}\times\{1 + [2\pi\chi^{(3)}E^2/(1 + 4\pi\chi^{(1)})]\} = n_0 + (2\pi\chi^{(3)}E^2/n_0)$, or

$$n = n_0 + n_2 I_0, \quad (1)$$

where $n_0 = (1 + 4\pi\chi^{(1)})^{0.5}$ is the refractive index at low light intensity (for TCE and PVC n_0=1,5); $n_2 I_0$ is the contribution of the third-order nonlinearity at the laser irradiation with intensity I_0 at $z=0$. According to Equation 1, the refractive index increases or decreases depending on the n_2 sign. The optical absorption at z=0 increases and includes the linear (α_0) and nonlinear (β) terms:

$$\alpha = \alpha_0 + \beta I_0 \quad (2)$$

The nonlinear characteristics $n_2 I_0$ and βI_0 were evaluated from the dependence of light transmission on the distance from the focal point. When n_2 has a positive value, the sample acts as the additional focusing lens (Fig. S1). When the sample is located in the –z range, the beam diameter in the aperture zone increases, which results in a decrease in the beam light portion transmitted through the aperture to the photodetector. When the sample is moved to the +z range, an additional focusing of light by the sample leads to a decrease in the beam diameter in the aperture plane and, hence, to an increase in the beam portion transmitted through the aperture. Therefore, z-scan T_{CA} curves recorded by a photodetector have a minimum in the pre-focal domain and a maximum in the post-focal domain. Figure 8a shows the T_{CA} dependence on the distance to the focal point (z

= 0) for composites of **(1)** with PVC (4% wt of complex **(1)**) prepared from a fresh solution of complex **(1)** in TCE and subjected to three cycles of heating to 70°C and slow cooling to 5°C with further aging for 48 h. It should be noted that the nonlinear response arises only after cyclic thermal treatment of the solution in TCE. Experimental values were approximated by the following theoretical dependence[41,42]

$T_{CA} = 1 - 4\Delta\Phi_0 x/[(x^2+1)(x^2+9)]$ (3)

Here, $x = z/z_0$ is the relative distance from the cell to the focal point; $z_0 = n_0\pi w_0^2/\lambda$ is the Rayleigh range, which is known to correspond to the distance from the focal point to the position where the beam radius equals $w_0\times(2)^{0.5}$; and $w_0$is the beam radius at the lens focal point. The approximation was made by fitting $\Delta\Phi_0$ and w_0 parameters. The best fit (solid line in Fig. 8a) corresponds to theoretical curve 1 at $\Delta\Phi_0 = 0.1$ and $w_0 = 20{,}6$ μm.

The imaginary part of the susceptibility can be found from the open-aperture transmittance (T_{OA}).

Figure 8b shows the T_{OA}– z dependence, where experimental data are approximated with the following theoretical expression (solid line)[41,42]:

$T_{OA} = [\ln(1 + q_0/(1 + x^2))]/[q_0/(1 + x^2)]$ (4)

According to the known equations

$n_2 I_0 = \Delta\Phi_0\lambda/2\pi L_{eff}$ (5)

$\beta I_0 = q_0/L_{eff}$, (6)

$n_2 I_0 = 0.002$ (when L_{eff} =7 μm). The value of I_0 under these conditions is 6.92×10^8W/cm^2, therefore, $n_2 = 3.4\times10^{-12}$. The real part of the third-order susceptibility is related to n_2 by formula $\chi^{(3)} = n_2 \times (n_0^2/0.0394)$. When n_0 is 1.5 (TCE, PVC), $\chi^{(3)} = 1.93\times10^{-10}$esu.

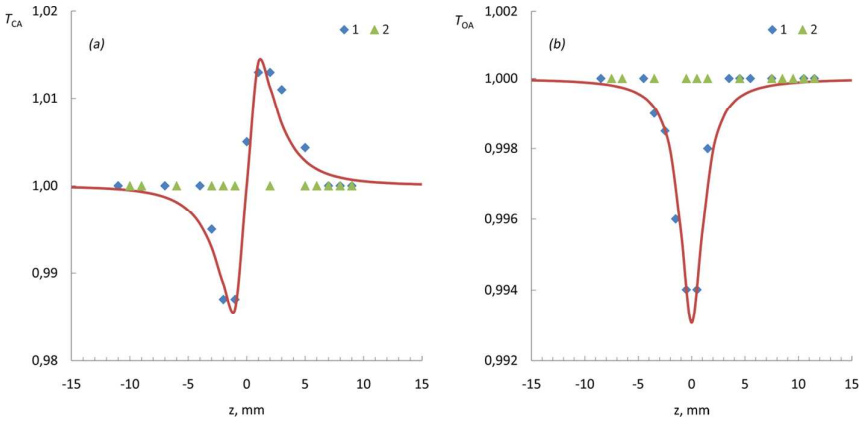

Fig. 8 Z-scan curves measured with (*a*) closed and (*b*) open aperture using a femtosecond laser. Samples were prepared from a solution of **(1)** in TCE subjected to three cycles of heating to 70°C and slow cooling to 5°C (1) and from a fresh solution (2). Composites contain PVC and complex **(1)** (4% wt).

The imaginary part of the susceptibility found from the open-aperture transmittance experiment (Fig. 8b) corresponds to the best approximation when $q_0 = 0.012$ and parameter β calculated from equation 6 is 2.5×10^{-8}. The imaginary part of the third-order susceptibility is related to factor β by formula $\chi^{(3)} = (\beta\lambda/4\pi)\times(n_0^2/0.0394)$ and its value corresponds to $\chi^{(3)} = 1.2\times10^{-11}$esu.

Thus, the total third-order susceptibility is determined namely by the real part and equals to $\chi^{(3)} = \{[\mathrm{Re}\chi^{(3)}]^2 + [\mathrm{Im}\chi^{(3)}]^2\}^{0.5} = 1.94\times10^{-10}$esu.

The T_{OA}– *z* dependences were also measured in the nanosecond range. Figure 9 shows the dependence of the relative quenching of the laser beam on the incident energy at z = 0 measured in samples prepared from a fresh solution of complex **(1)** in TCE, as well as from solutions subjected to three cycles of heating to 70°C and slow cooling to 5°C.

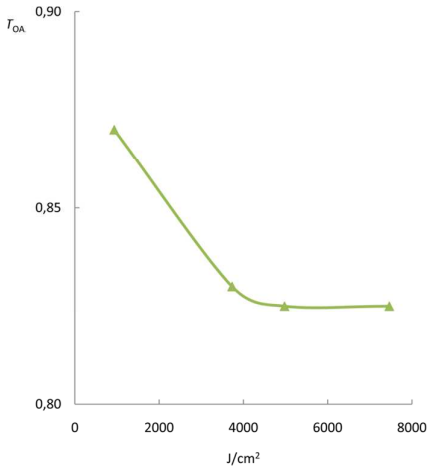

Fig. 9 Dependence of optical transmission with open aperture T_{OA} on the incident energy at z = 0 measured in samples prepared from a solutions subjected to three cycles of heating to 70°C and slow cooling to 5°C.

A decrease in the optical transmission of the sample at high incident energies is observed. Although the value of this decrease is not very high (only 0.82 at an incident energy of about 4000 J/cm^2), this observation reveals the perspectives of further application of the proposed methodology for fabrication of nonlinear optical supramolecular materials containing well-defined crystalline nanoparticles constructed from crownphthalocyaninates and incorporated into polymeric matrixes.

Conclusions

The detailed investigation of the structure and the optical behavior of ruthenium(II) tetra-15-crown-5-phthalocyaninate containing axially coordinated molecules of pyrazine was carried out. The features of self-assembling of complex in TCE solution, thin films and polymeric composites with polyvinylcarbazole were revealed. It was found that the nonlinear response of composites arises only after cyclic thermal treatment of the solution in tetrachloethane and storage up to 48 h. At the same time, it has been demonstrated that the crystal lattice of ruthenium(II) crown-phthalocyaninate contains numerous weak contacts (CH…π, CH…N, CH…O, CH…Cl), which are responsible for the formation of nanoparticles in high-boiling solvents, as well as in polymeric films. Anisotropy of optical properties of these compounds is determined by architecture of ensembles and nanoparticles, whose size and geometry depend on the number and duration of heating/cooling cycles as well as aging time. Hence, it confirms that self-assembling has essential effect on the nonlinear optical behavior of the ruthenium Pc polymeric composites.

It is expected that the developed methodology, can be used for preparation of novel efficient composite optical limiters starting from other crownphthalocyaninates. Among them there might be trivalent metal tetra-15-crown-5-phthalocyaninates, whose nonlinear optical properties have been previously investigated only in TCE solution. For example, it was shown that gallium(III) or yttrium(III) tetra-15-crown-5-phthalocyaninates have the values $\chi^{(3)} = (3\pm1) \times 10^{-10}$ esu[20,25] while indium(III) tetra-15-crown-5-phthalocyaninate has increased $\chi^{(3)}$ value up to 13.4×10^{-10} esu.[21] However, thermally induced self-assembly in solution of these complexes followed by fabrication of polymeric has not been studied and its influence on their nonlinear optical properties would be the object of our further investigation.

Acknowledgements

We gratefully acknowledge support from the Russian Foundation for Basic Research (project nos. 14-03-00049_a and 14-03-00977_a) and OPTEC LLC (Contract № 49/2014/75-Msk). The authors are grateful to Dr. S.S. Abramchuk (INEOS RAS) for help with TEM experiments.

Notes and references

1. G. de la Torre, P. Vazquez, F. Agullo-Lopez, and T. Torres, *Chem. Rev.*, 2004, **104**, 3723–3750.

2. M. Calvete, G. Y. Yang, and M. Hanack, *Synth. Met.*, 2004, **141**, 231–243.

3. M. Nicolau, G. Rojo, T. Torres, and F. Agulló-López, *J. Porphyrins Phthalocyanines*, 1999, **3**, 703–711.

4. L. Yang, Z. Chen, S. Zhang, L. Niu, C. Tung, Y. Chi, J. Xiang, and F. Zhang, *Dyes Pigm.*, 2014, **102**, 251–256.

5. M. K. Casstevens, M. Samoc, J. Pfleger, and P. N. Prasad, *J. Chem. Phys.*, 1990, **92**, 2019–2024.

6. J. M. Fox, T. J. Katz, S. Van Elshocht, T. Verbiest, M. Kauranen, A. Persoons, T. Thongpanchang, T. Krauss, and L. Brus, *J. Am. Chem. Soc.*, 1999, **121**, 3453–3459.

7. S. Fang, H. Tada, and S. Mashiko, *Appl. Phys. Lett.*, 1996, **69**, 767–769.

8. J. J. Doyle, J. Wang, S. M. O'Flaherty, Y. Chen, A. Slodek, T. Hegarty, L. E. Carpenter II, D. Wöhrle, M. Hanack, and W. J. Blau, *J. Opt. A Pure Appl. Opt.*, 2008, **10**, 075101.

9. S. Tekin, U. Kürüm, M. Durmuş, H. G. Yaglioglu, T. Nyokong, and A. Elmali, *Opt. Commun.*, 2010, **283**, 4749–4753.

10. J. Britton, C. Litwinski, E. Antunes, M. Durmuş, V. Chaukea, and T. Nyokong, *J. Macromol. Sci. Part A*, 2013, **50**, 110–120.

11. M. Yüksek, A. Elmali, M. Durmuş, H. Gul Yaglioglu, H. Ünver, and T. Nyokong, *J. Opt.*, 2009, **12**, 015208.

12. J. Britton, M. Durmuş, V. Chauke, and T. Nyokong, *J. Mol. Struct.*, 2013, **1054-1055**, 209–214.

13. C. Mkhize, J. Britton, and T. Nyokong, *Polyhedron*, 2014, **81**, 607–613.

14. K. E. Sekhosana, E. Amuhaya, and T. Nyokong, *Polyhedron*, 2015, **85**, 347–354.

15. K. Sanusi and T. Nyokong, *J. Photochem. Photobiol. A Chem.*, 2015, **303-304**, 44–52.

16. Y. G. Gorbunova, A. G. Martynov, and A. Y. Tsivadze, in *Handbook of Porphyrin Science*, eds. K. M. Kadish, K. M. Smith, and R. Guilard, World Scientific Publishing, 2012, vol. 24, pp. 271–388.

17. A. G. Martynov, Y. G. Gorbunova, and A. Y. Tsivadze, *Russ. J. Inorg. Chem.*, 2014, **59**, 1627–1656.

18. A. D. Grishina, Y. G. Gorbunova, V. I. Zolotarevsky, L. Y. Pereshivko, Y. Y. Enakieva, T. V. Krivenko, V. Savelyev, A. V. Vannikov, and A. Y. Tsivadze, *J. Porphyrins Phthalocyanines*, 2009, **13**, 92–98.

19. A. V. Vannikov, Y. G. Gorbunova, A. D. Grishina, and A. Y. Tsivadze, *Prot. Met.*, 2013, **49**, 57–65.

20. A. V. Vannikov, A. D. Grishina, Y. G. Gorbunova, T. V. Krivenko, A. S. Laryushkin, L. A. Lapkina, V. Savelyev, and A. Y. Tsivadze, *Polym. Sci. A*, 2011, **53**, 1069–1075.

21. A. D. Grishina, Y. G. Gorbunova, T. V. Krivenko, L. A. Lapkina, V. V. Savel'ev, A. V. Vannikov, and A. Y. Tsivadze, *Prot. Met.*, 2014, **50**, 472–479.

22. S. L. Selektor, V. V. Arslanov, Y. G. Gorbunova, O. A. Raitman, L. S. Sheinina, K. P. Birin, and A. Y. Tsivadze, *J. Porphyrins Phthalocyanines*, 2008, **12**, 1154–1162.

23. S. L. Selektor, A. V. Shokurov, V. V. Arslanov, Y. G. Gorbunova, K. P. Birin, O. a. Raitman, F. Morote, T. Cohen-Bouhacina, C. Grauby-Heywang, and A. Y. Tsivadze, *J. Phys. Chem. C*, 2014, **118**, 4250–4258.

24. L. A. Lapkina, N. Y. Konstantinov, V. E. Larchenko, Y. G. Gorbunova, and A. Y. Tsivadze, *J. Porphyrins Phthalocyanines*, 2009, **13**, 859–864.

25. A. V. Vannikov, A. D. Grishina, Y. G. Gorbunova, V. I. Zolotarevskii, T. V. Krivenko, A. S. Laryushkin, L. A. Lapkina, V. V. Savel'ev, and A. Y. Tsivadze, *High Energy Chem.*, 2015, **49**, 36–43.

26. A. D. Grishina, F. Y. Konnov, Y. G. Gorbunova, Y. Y. Enakieva, L. Y. Pereshivko, T. V. Krivenko, V. Savelyev, A. V. Vannikov, and A. Y. Tsivadze, *Russ. J. Phys. Chem. A*, 2007, **81**, 982–989.

27. A. D. Grishina, Y. G. Gorbunova, Y. Y. Enakieva, T. V. Krivenko, V. Savelyev, A. V. Vannikov, and A. Y. Tsivadze, *High Energy Chem.*, 2008, **42**, 297–304.

28. Y. Y. Enakieva, Y. G. Gorbunova, S. G. Sakharov, and A. Y. Tsivadze, *Russ. J. Inorg. Chem.*, 2002, **47**, 1815–1820.

29. G. R. Fulmer, A. J. M. Miller, N. H. Sherden, H. E. Gottlieb, A. Nudelman, B. M. Stoltz, J. E. Bercaw, and K. I. Goldberg, *Organometallics*, 2010, **29**, 2176–2179.

30. I. Horcas, R. Fernández, J. M. Gómez-Rodríguez, J. Colchero, J. Gómez-Herrero, and a M. Baro, *Rev. Sci. Instrum.*, 2007, **78**, 013705.

31. G. M. Sheldrick, *SADABS, Bruker AXS Inc.*, Madison, WI-53719, USA, 1997.

32. *SMART V5.051 and SAINT V5.00, Area detector control and integration software, Bruker AXS Inc.*, Madison, WI-53719, USA, 1998.

33. G. M. Sheldrick, *SHELXTL-97 V5.10, Bruker AXS Inc.,* Madison, WI-53719, USA, 1997.

34. Y. G. Gorbunova, Y. Y. Enakieva, S. G. Sakharov, and A. Y. Tsivadze, *J. Porphyrins Phthalocyanines*, 2003, **07**, 795–800.

35. Y. Y. Enakieva, Y. G. Gorbunova, S. E. Nefedov, and A. Y. Tsivadze, *Mendeleev Commun.*, 2004, **14**, 193–194.

36. L. A. Lapkina, Y. G. Gorbunova, S. E. Nefedov, and A. Y. Tsivadze, *Russ. Chem. Bull., Int. Ed.*, 2003, **52**, 1633–1636.

37. A. G. Martynov, O. V. Zubareva, Y. G. Gorbunova, S. G. Sakharov, S. E. Nefedov, F. M. Dolgushin, and A. Y. Tsivadze, *Eur. J. Inorg. Chem.*, 2007, 4800–4807.

38. M. Capdevila-Cortada, J. Castelló, and J. J. Novoa, *CrystEngComm*, 2014, 8232–8242.

39. M. Kasha, H. R. Rawls, and M. A. El-Bayoumi, *Pure Appl. Chem.*, 1965, **11**, 371–392.

40. S. Yanagisawa, T. Yasuda, K. Inagaki, Y. Morikawa, K. Manseki, and S. Yanagida, *J. Phys. Chem. A*, 2013, **117**, 11246–53.

41. M. Sheik-Bahae, A. a. Said, T.-H. Wei, D. J. Hagan, and E. W. Van Stryland, *IEEE J. Quantum Electron.*, 1990, **26**, 760–769.

42. R. L. Sutherland, *Handbook of Nonlinear Optics,* Marcel Dekker, New York, Marcel Dek., 1996.